



DESIGN AND DEVELOPMENT OF A LOW-COST SENSOR IOT COMPUTING DEVICE FOR GREENHOUSE GAS MONITOR FROM SELECTED INDUSTRY LOCATIONS

IBRAHIM HAMIDU *, BENJAMIN AFOTEY † AND ZAKARIA AYATUL-LAHI‡

Abstract. The objective of the study is to develop low-cost IoT based sensor to monitor real-time greenhouse gases (GHG) emissions data from selected industry locations (city blocks) in a top-down approach. Three (3) industry locations were selected within the Suame Industrial complex (the largest single cluster of artisanal engineering and light manufacturing in Sub Saharan Africa and even Africa) which has no reported GHG emissions data. A GHG monitor was developed using Atmega328 microcontroller and a sim800I GSM module was used to collect a 24-hour real-time minute-by-minute emissions data from the selected industry locations. A MQ-4 (methane/natural gas sensor), MQ-135 (Nitrous Oxide sensors) and DHT22 (temperature and humidity sensor) were used in the GHG monitor design. The GHG of concern were carbon dioxide, methane and nitrous oxide. A total of 3627 emissions data were collected and analyzed from the three (3) industry locations. Location 3 had the highest average carbon dioxide emissions of 508.11 ppm, followed by location 2 with 477.31 ppm with the least emissions in location 1 with 472.51 ppm which are above the global carbon dioxide average of 414.7 ppm. The average methane emission was highest in location 1 with 0.1599 ppm (1599 ppb), followed by location 3 with 0.1366 ppm (1366 ppb) with the least average methane emission of 0.1358 ppm (1358 ppb) in location 2 which are slightly below the global methane average of 1895.7 ppb. The MQ-135 nitrous oxide sensor reported zero emissions data throughout the deployment at the various industry locations which indicated the nitrous oxides emission in the selected sample site is negligible or below the detectable range of the sensor.

Key words: Low-cost-sensor IoT design, GHG monitor, Real-time emissions data, Regression Analysis, Ghana.

AMS subject classifications. 68M14, 68M18

1. Introduction. Greenhouse gases (GHG) are considered the main contributor to global warming and climate change [1] but the inefficiencies in methods used in the GHGs estimation has created huge emissions and sink data gaps. Numerous Sub Saharan African countries such as Ghana lack the capacity to effectively conduct Air Quality monitoring and meeting the Air Quality standards [10].

An estimated 75% of people in developed countries live in cities as compared to 35 % of people in developing countries [24]. There is a projected increase in urban (city) dwellers, with an estimated 66% of the total human population living in cities by 2050 [11]. The movement of majority of the population into urban cities will lead to significant increase in energy demand [11] and a drastic increase in air pollution within Sub-Saharan Africa [25]. Greenhouse Gases which are air pollutants absorb and radiate heat back to the earth surface increasing the atmospheric temperature [21].

Air pollution which result from the release of harmful solid, liquid or gaseous suspended particles has been estimated to cause over 28,000 deaths in Ghana in 2018 [25]. Findings suggest that among the impact of climate change in Ghana, there is a high temperature projection and low rainfall in the years 2020, 2050, and 2080 and a projected desertification rate of 20,000 hectares per annum [4].

The main estimation approaches of GHG estimation are the bottom-up and top-down approaches. Top-down approach involves direct ambient or atmospheric emissions concentration measurement whereas bottom-up approach involves the direct emissions measurement from the individual emissions sources [2]. The EPA in Ghana, responsible for the monitoring and reporting of GHG emissions uses the IPCC 2006 guidelines and software with National and international GHG inventory system [5]. The IPCC 2006 guidance is based on

*Department of Chemical Engineering, Kwame Nkrumah University of Science and Technology, Private Mail Bag, University Post Office, KNUST – Kumasi, Ghana (hamiduibrahim75@gmail.com)

†Department of Chemical Engineering, Kwame Nkrumah University of Science and Technology, Private Mail Bag, University Post Office, KNUST – Kumasi, Ghana. (afotey_benjamin@hotmail.com).

‡Private Research, ZAKS Electronics, Post Office Box WE 586, Asawase Kumasi, Ghana (ayatullahizakaria@gmail.com)

bottom-up models (activity and impact factor based) which requires several assumptions and yields uncertainties in the results.

Low Cost Sensors (LCS) over time have experienced tremendous developments and application in greenhouse gas accounting and reporting at lower levels (city blocks) [31]. However, the use of low cost sensor in Ambient Air Quality monitoring is limited to Particulate matter only in Ghana evidenced in the Ghana Urban Air Quality Project (GHAir) [10, 25]. The use of the low cost sensors in the GHAir project has also faced limitations in reporting monitored data due to poor Wi-Fi connectivity and power supply in deployed areas [25].

The objective of this research is to determine ambient greenhouse gases within selected industry locations within the Suame Industrial Complex using a Top-Down approach. In this research study, a low-cost-sensor IoT based GHG monitor to report real-time GHG emissions data was designed and developed. The developed monitor was then deployed within selected industry locations within the Suame Industrial Complex to collect a 24-hour minute-by-minute GHG emissions data. A statistical tool (Minitab Statistical Software 20.3 (64 bit)) was used in analyzing reported/collected GHG emissions data.

2. Literature Survey. The phenomenon of air pollution falls under SDG 3 – Good Health and Wellbeing and specifically SDG 3.9. SDG 3.9 targets the substantial reduction in illnesses and death associated with the release of hazardous pollutants. Air pollution also affects SDG 11 – Sustainable Cities and Communities, and Specifically Target 11.6. Target 11.6 emphasizes the reduction of the environmental impacts of cities on people to enhance a safe and inclusive human settlement [25]. Greenhouse Gases such as Ozone, Methane, Carbon Dioxide, Nitrous Oxide, and Water Vapour absorb and emit radiant energy in the earth atmosphere within the Thermal Infrared Spectrum/region [21]. Greenhouse gases are predominantly made of Carbon Dioxide and Methane [32] and are emitted/released mostly through human-made (anthropogenic) activities mainly associated with fossil fuel use [21]. The absorption and emission of radiant energy leads to Greenhouse effect which in excess can lead to catastrophic effect due to increase in atmospheric temperature to unbearable limits [21]. Anthropogenic methane sources account for 60% whereas Natural gas sources account for 40% of the global methane emissions [18].

The uncertainty of CO₂ emissions from Land Use according to the 4th Assessment Report is estimated at ± 2933 MtCO₂ at the 1990 global level [33] with an average temperature increase over land by $1.320.04^{\circ}C$ [34]. The average temperature increase of the ocean is also estimated as $0.590.006^{\circ}C$ [34]. The increase in atmospheric temperature poses a threat to aquatic and human survival [32]. There has been an estimated atmospheric temperature increase of $0.7^{\circ}C$ from 1961 to 1990 [34].

Carbon Dioxide is the highest contributor to Global Warming and the most significant greenhouse gas [13]. The concentration of Carbon Dioxide increased from 280 ppm at a pre-industrial level value to 410 ppm in 2020 [35]. Although the methane increase within the atmosphere which constitute 16% of GHG emissions is not as high as carbon dioxide, it however contributes as much as carbon dioxide due to its Global Warming Potential [18]. Without the Greenhouse effect, the earth atmospheric temperature will be at an unbearable $-18^{\circ}C$ [21], and in excess (due to the drastic increase in GHG concentration) will also lead to unbearable high atmospheric temperature. Although the global GHG emissions slowed after 2014, the emissions generally increased from 2010 to 2018 and peaked at 58 GtCO₂eq in 2018, 11% above 2010 levels [36, 37].

In order to mitigate the effects of greenhouse gases due to sustained increase in GHG emissions, several international agreements have been formed. Among them is the Paris agreement which seek to limit the global atmospheric temperature increase to $2^{\circ}C$ and possibly $1.5^{\circ}C$ above preindustrial era levels [36]. Among the estimation techniques used in GHG accounting are the top-down and bottom-up approaches.

Top-down estimates uses meteorological data like wind speeds and directions to obtain emissions data through inverse modeling by projecting atmospheric transportation. Inverse modelling is based on source-receptor relationship atmospheric data based [38]. The Top-down approach which monitors the atmospheric emissions provides an emissions aggregate from a location but does not identify emissions sources unless tracers are identified for specific emissions [2].

Bottom-up analysis includes life-cycle analysis [39]. Bottom up estimation is from emissions inventory which are heterogeneous from one location to another and prone to uncertainties, errors and manipulations. An example of the bottom-up approach is the emissions factor approach as used in the IPCC guidelines [38].

The emissions data on the global scale reported by countries using the bottom-up approach is approximately less than half of the emissions data from the top-down approach [38]. Omissions of emissions sources account for the weakness of the bottom up approach [2].

The effectiveness of the GHG accounting and reporting methodologies rely on drivers and motives which are characterized by the level of development of a country - whether a country is develop or developing. Developed country have much obligations to gather, validate, model data and used in estimating and reporting whereas developing countries have voluntary obligation and most lack the required data. The outcome of GHG accounting and reporting in developing countries is characterized by the lack of necessary data, expertise, resources to enhance the effective evaluation of GHG. Lack of the up to date generation data also makes the results from the various models used in GHG accounting and reporting incoherent [40].

Among the four main GHG (bottom-up) accounting methodologies are the IPCC method for national accounting, corporate level accounting (municipalities), Life Cycle Analysis/Assessment and Carbon Trading methodologies. The results from these methods varies significantly when applied to the same activity and geographies based on the assumption made [40].

Model based GHG estimation (GHG accounting and Reporting) such as the IPCC method is widely accepted. The Tier-1 of the IPCC model is used for national inventory reporting [5] whereas the Tier-2 can be applied to various sub sectors such as emissions from waste sources [41]. Other models such as the LandGEM method and the Triangular method were applied by [41] in estimated landfill gas (methane).

The authors of [31] assessed in their research the adaptation of the IPCC model for small cities in carbon monitoring. In their research, the use of the IPCC model was asserted as ineffective in estimating carbon emissions on small cities level due to lack of timely real time monitoring data. Lack of intelligent energy monitoring system (due to high cost) to monitor and report carbon inventory data was identified among the limitation of adapting the IPCC model for small cities. The last identified limitation is the inability to universally adapt the IPCC model for different levels in small cities due to the differences in estimation method of monitoring data and long term data [31].

Among the development in the monitoring of GHG within the earth atmosphere in recent times involved the use of Satellites. Satellites are used to fill the spatial GHG monitoring gaps within the earth's atmosphere. The Thermal And Near infrared Sensor for Carbon Observation (TANSO) launched by Japan in 2009 which aboard Greenhouse gases Observing SATellite (GOSAT) was the first satellite instrument designed specifically to record methane and Carbon Dioxide concentrations [13]. Other satellites such as the Orbiting Carbon Observatory - 2 (OCO-2) launched by NASA in 2014 and the TanSat (also known as CarbonSat) launched by the Chinese Space Program in 2016 are dedicated to monitor GHG (carbon dioxide) in the Earth's atmosphere [35]. Other instruments such as the SCanning Imaging Absorption spectroMeter for Atmospheric CHartographY (SCIAMACHY) launched in 2002 and lost in 2012 by the European Space Agency (ESA) which aboard the ENVironmental SATellite (ENVISAT) could retrieve GHG concentrations [13].

Low Cost Sensors (LCS) are characterized by their low purchase pricing and operation cost as compared to the purchase and operating cost of other sensors/analyzers [17]. Among the LCS are the electrochemical gas sensors, semiconducting gas sensors, and the optical particle monitors [17, 21].

One of the main advantages and motivations for using Low Cost Sensors is in spatial resolution increase of Ambient air quality. This enhances the detection of variability below a regional/city level, to lower levels such as city-block or below. The size and low cost of sensors provides the opportunity for deploying in small footprint locations and in mobile/semi-mobile sampling schemes. Current models techniques cannot compete at lower levels of spatial resolutions due to high dynamic variability of the pollutants, and external hindrances such as wind, humidity etc... which is overcome by the use of LCS. Mostly Low Cost Sensors marketed as a single pollutant sensor exhibit cross-sensitivity to other pollutants [8].

Among the various approach used in sensor selectivity are temperature, filters, catalyst and specific adsorption. Temperature changes affects the spontaneity/rate of a reaction (the activity of a reducing agent) thereby affecting the selectivity of the sensor. Methane burns at high temperature compared to the low temperature (room temperature) at which CO and hydrogen burns. Hence at elevated temperatures (high above room temperature) at which the gases burn rapidly, it is likely gases such as hydrogen and CO will not be detected [42].

Specific materials that allow specific gases to react can be used to enhance sensor selectivity. Hygroscopic salts are used to attract/concentrate water for humidity sensors. Another example is the use of sulfanilic acid to enhance the selectivity of NO₂ [42].

Metal Oxides as used in sensor development varies the surface conductance in a gaseous atmosphere. Various metal oxides are used as catalyst or dopants to enhance to response to some specific gases. Tin oxide (which is the most studied material) modifies the response spectrum of the sensor to gases by enhancing suitable changes of the catalyst or dopant deposited. Among the dopants/catalyst are palladium, platinum and cadmium [43].

3. Materials and Methods.

3.1. Selected Sample Site. The selected sample site for this project is the Suame Industrial Complex. The Suame Industrial Complex mainly known as Suame Magazine comprises over 12,000 enterprises and over 200,000 artisans involved in operations such as equipment and machinery manufacturing, foundries, vehicle repairs, materials workings etc. The Suame Magazine spans 900,000 square meters, 1.8 km long and 0.32 km wide with an estimated cluster nucleus perimeter of 7 km. [3, 14, 20, 29].

Three (3) industry locations were selected within the selected sample site. The selected location 1 (Lat: 6.7211, Long: -1.6291) is the Abu-Dia Company Limited with operations in metal foundry. Location 2 (Lat: 6.7113, Long: -1.6306) is KOSAMO Limited with operations in HVAC operations and duct fabrication. Location 3 (Lat: 6.7117, Long: -1.6422) is Presank Company Limited with operations in waste handling and recycling.

3.2. Selected pollutants of concern. This project is limited to Carbon Dioxide, Methane and Nitrous Oxide due to the quantities release and their potency in trapping heat within the earth atmosphere

Carbon dioxide can potentially be produced from methane oxidation [22] and is the most oxidized state of Carbon, which is used as a chemical reagent and a phosgene substitute [44]. The average global carbon dioxide emissions level in 2021 was 414.7 ppm, a 2.66 ppm increase from the 2020 average. A 35 billion tons of carbon dioxide were emitted into the atmosphere in 2021, and these carbon dioxide emissions have the potential of trapping heat within the atmosphere for thousands of years [23].

Methane is a stable gas which starts decomposing into elements at 785°C [45]. A graph of the average global methane emissions per year is shown. As observed by [23], the global average methane emissions in 2021 was 1895.7 ppb, a 15% higher than the 1984 – 2006 period and a 162% higher than the pre-industrial level. The methane atmospheric residence time is about 9 years but is 25 times more potent in trapping heat in the atmosphere, and a short-term climate change influencer as compared to carbon dioxide [23].

Nitrous Oxide is a colourless, slightly pleasant sweet odour and taste and non-flammable gas which is acknowledged as an undesired by-product in exhaust gases from lean NO_x trapping [15]. Agriculture dominates the global anthropogenic sources of N₂O [22]. Among the sources of Nitrous Oxide are industries, fertilizer production, and wastewater treatment plant [15, 28]. Nitrous Oxide is currently the largest destroyer of ozone in the stratosphere than any other reactive chemical [28]. The Global Warming Potential of Nitrous Oxide is between 265 to 298 over a 150 years' time series [15].

3.3. Development of an IoT GHG monitor. The block diagram of the monitor design is shown in figure 3.1. The various components including the sensors used in the monitor design and development are shown in figure 3.2. The sensors used in this project are MQ-135 (nitrous oxide sensor), MQ-4 (methane sensor), SCD-30 (carbon dioxide, temperature and humidity sensor), and DHT22 (temperature and humidity sensor).

MQ-135 is a Tin Dioxide (SnO₂) semiconductor based gas sensor effective in detecting Nitrous Oxide, Ammonia, Benzene, Smoke, alcohol and Carbon Monoxide [1, 21]. MQ-4 is composed of Al₂O₃ ceramic tube, Tin Dioxide (SnO₂) sensitive layer, measuring electrode and heater that detects the concentration methane/natural gas between 0 ppm - 10000 ppm [6].

Sensiron SCD-30 operates on the non-dispersive infrared (NDIR) principle which measures CO₂ between 0 - 40000 ppm (± 30 ppm + 3 % accuracy for range between 400 ppm – 10000 ppm), temperature between - 40 to 120 °C, and relative humidity between 0 % - 100 % [19]. NDIR sensors measure the CO₂ levels by measuring the amount of infrared light reflected by the CO₂ [9].

DHT22 contains a thermistor for dry bulb temperature measurement and a capacitive sensor for moisture/humidity measurement. The DHT22 measures temperature between -40 to +80 °C (0.5 °C accuracy)

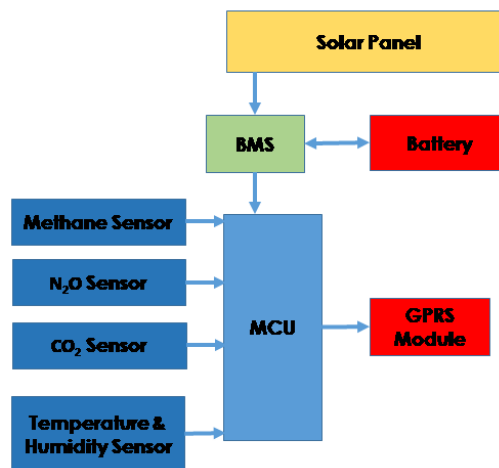


Fig. 3.1: Block diagram of the various units of the GHG monitor

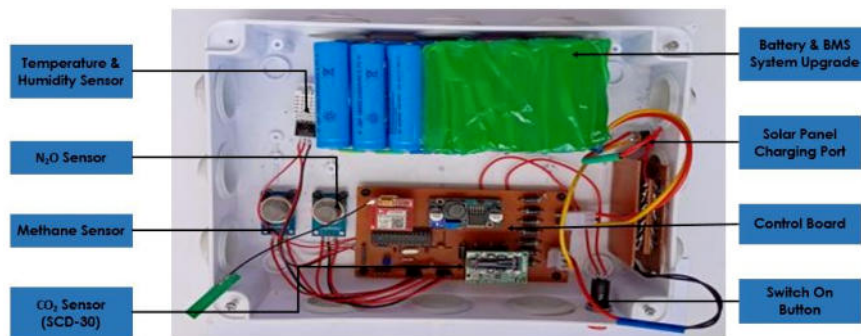


Fig. 3.2: Various components in the developed monitor

and relative humidity from 0% to 100% (2% accuracy) [46, 47].

The DHT22 sensors measure 4% more accurate temperature readings and 18% more accurate humidity readings than its DHT11 [48]. The various sensors were calibrated using libraries from the sensor manufacturers designated for the working conditions of the sensors based on the various location. The calibration of the sensor was to enhance better performance and to enhance the accuracy of the monitored emissions.

Among the other various components includes;

1. Battery pack (19.6 Ah)
2. A battery Management System
3. A 50 W solar panel
4. An Atmega 328 microcontroller unit
5. A sim800I GSM module
6. Im2596 buck converter
7. A 28 pin IC socket
8. 1N5408
9. A 2.54 male and female pin headers
10. 16 MHz crystal
11. A 22 Pico farad, 100 Nano farad capacitors

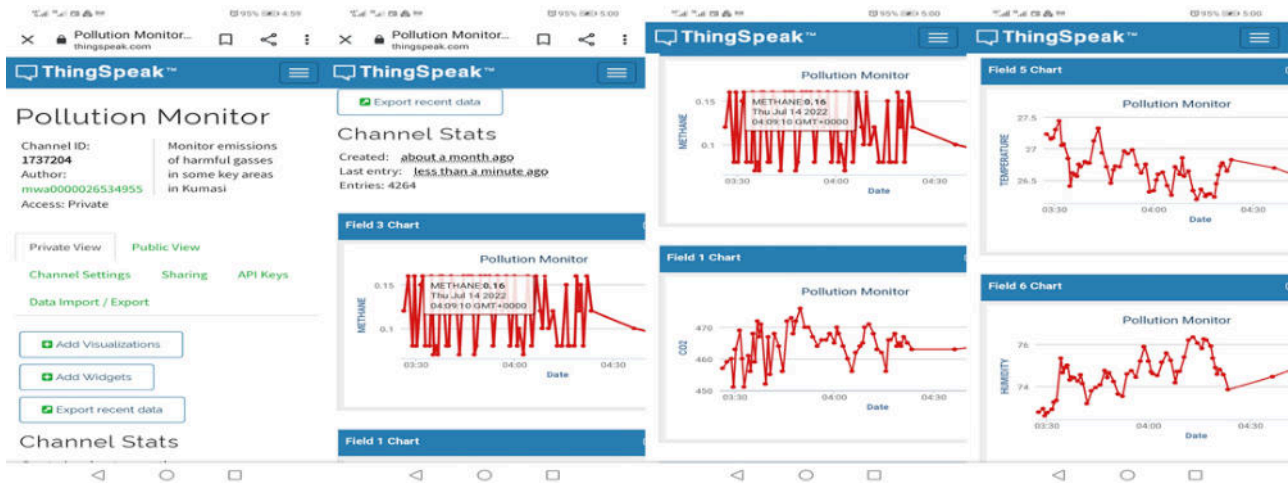


Fig. 3.3: Various components in the developed monitor



Fig. 3.4: Images of the deployment at a. location 1 (lat: 6.7211, long: -1.6291); b. Location 2 Images of the deployment at a. location 1 (lat: 6.7211, long: -1.6291); b. Location 2

12. 10 k ohms, 20 k ohms, and a 1 k ohm resistors
13. A Vh3.96 connector

The sim800I GSM module was integrated into the monitor to enhance the transmission of the monitored emissions data onto a Thing Speak cloud platform. The Thing Speak (by Mathworks) IoT analytic platform was selected for this project due to the easiness in data download from the platform, easy monitoring and visualization of live reported data on the platform. A private access was created. Screenshots of the mobile view interface of the ThingSpeak cloud platform is shown in figure 3.3.

3.4. GHG monitor deployment. The developed monitor was deployed in location 1 (Lat: 6.7113, Long: -1.6306) from 2022-07-19 (18:00:10 GMT) to 2022-07-20 (17:59:42 GMT) and a total of 1286 data collected within the 24 hours' deployment. The monitor was then deployed in location 2 (Lat: 6.7211, Long: -1.6291) with 1246 total data collected within 24 hours deployed period. The developed was lastly deployed at location 3 (Lat: 6.7117, Long: -1.6422) with 1095 data collected in the 24 hours deployed period. Imaged of the monitor deployed in location 1,2 and 3 is shown in figure 3.4.

3.5. Statistical analysis of collected GHG emissions data. Among the statistical analysis performed on the collected data are descriptive statistics analysis, Time series plots, Surface plots, Correlation and Regression analysis of the data.

A correlation coefficient (r) as used in correlation analysis is the measure of the linear relationship between two (2) variables. The Pearson product-moment correlation coefficient (r) is a parametric measure of the linear association of normal distribution between two (2) variables. Conversely to the Pearson coefficient. [26].

Monitored environmental factors (temperature and humidity) are correlated with the monitored greenhouse

Table 4.1: Summary of descriptive statistics of reported pollutant emissions data by the various selected sensors in various locations.

Location (Lat, Long)	Descriptive Statistics	Pollutant/Analyte (ppm)		
		CO2 (SCD-30)	CH4 (MQ-4)	N2O (MQ-135)
Location 1 (Lat, Long)	Mean	472.51	0.1599	0
	Min	421.00	0.0800	0
	Max	513.00	0.5100	0
	Standard Deviation	11.59	0.08542	0
Location 2 (Lat, Long)	Mean	477.31	0.1358	0
	Min	435.00	0.0800	0
	Max	515.00	0.3700	0
	Standard Deviation	12.44	0.05857	0
Location 3 (Lat, Long)	Mean	508.11	0.1366	0
	Min	439.00	0.0800	0
	Max	585.00	0.4800	0
	Standard Deviation	11.43	0.05602	0

gases in this research study. Temperature and relative humidity were selected in the correlation investigation with the various emissions data due their influence in sensor performance and greenhouse gases concentration and pollutant chemistry as outlined in literature [8, 12, 16, 27, 30].

Regression Analysis is modeling of a set of numerical data using a set of methods and relates a dependent (response) variable to one or more independent (explanatory) variables [26].

Minitab Statistical Software 20.3 (64 bit) was the only statistical software used for all the data analysis. The listed analysis was done on the 3627 data collected in the final deployment.

The time-stamped minute-by-minute reported emissions data made it necessary to conduct time series plots of the reported emissions data from the various locations. The time series plot was also used to investigate performance of DHT22 and SCD-30 sensor.

4. Findings and Results.

4.1. Descriptive statistics of reported data. The descriptive statistics (mean, minimum value (min), maximum value (max) and the standard deviation) of the reported carbon dioxide, methane and nitrous oxide emissions data are shown in table 4.1. The descriptive statistics of the temperature and humidity reported values by the DHT22 and SCD-30 sensors are shown in table 4.2.

4.2. Correlation analysis. The effects of temperature and humidity was investigated on the monitoring of the greenhouse gases. As indicated in by [8] that these factors (temperature and humidity) affect sensor performance. The examination of temperature and humidity effects was also investigated on the dispersion or production/emission of carbon dioxide and methane as investigated in correlation analysis by [27] and [12]. The correlation analysis of carbon dioxide, and methane with temperature and humidity is shown in table 4.3.

4.3. Regression Analysis. Based on the correlation analysis as shown in table 4.2, regression analysis of carbon dioxide and methane (as response variable) against temperature and humidity (as independent) variable was investigated, with the corresponding coefficient of determination (R^2) as shown in table 4.4 and 4.5. The DHT22 sensors temperature and humidity data was used in all the regression analysis.

The regression analysis of temperature against humidity was investigated as shown in table 4.6.

4.4. Time Series Plots. Time series plot was used to visualize the reported emissions data. The time series plot of carbon dioxide and methane emissions data, and environmental factors (temperature and humidity) data for the various deployed locations are shown in figure 4.1 to 4.6 below.

Time series plot of reported data in location 1 (lat: 6.7211,-1.6291)

Time series plot of reported data in location 2 (lat: 6.7113, -1.6306)

Table 4.2: Summary of descriptive statistics of reported environmental factors data by the various selected sensors in various locations

Location (Lat, Long)	Descriptive Statistics	Environmental Factors			
		Temperature (o C)		Humidity (%)	
		(SCD-30)	(DHT22)	(SCD-30)	(DHT22)
Location 1 (Lat, Long)	Mean	28.20	26.47	62.91	70.57
	Min	24.40	22.90	37.79	36.50
	Max	36.48	33.90	75.97	87.50
	Standard Deviation	3.14	3.11	10.97	14.94
Location 2 (Lat, Long)	Mean	27.95	26.77	65.00	70.24
	Min	23.04	23.40	48.20	51.00
	Max	34.62	32.30	80.56	84.50
	Standard Deviation	3.34	2.56	10.07	9.99
Location 3 (Lat, Long)	Mean	30.69	28.20	62.51	72.62
	Min	27.65	25.30	39.58	46.00
	Max	40.01	35.40	71.77	85.80
	Standard Deviation	2.43	2.47	7.51	11.03

Table 4.3: Summary of correlation details from the various locations

95 % Confidence Interval Pearson Correlation			
Location Details		Temperature	Humidity
Location 1 (lat: 6.7211, long: -1.6291) 1286 Data	CO2	-0.258	0.252
	CH4	0.146	-0.144
	Temperature		-0.996
Location 2 (lat: 6.7113, long: -1.6306) 1246 Data	CO2	-0.704	0.696
	CH4	-0.097	0.113
	Temperature		-0.991
Location 3 (lat: 6.7117, long: -1.6422) 1095 Data	CO2	-0.234	0.258
	CH4	0.096	-0.074
	Temperature		-0.993

Table 4.4: Summary of regression analysis of carbon dioxide against temperature and humidity from the various deployed locations

Location details	Regression equation	R2 (%)
Location 1 (lat: 6.7211, long: -1.6291) 1286 Data	$CO_2 = 607.0 - 3.61 \times \text{Temperature} - 0.552 \times \text{Humidity}$	7.02
Location 2 (lat: 6.7113, long: -1.6306) 1246 Data	$CO_2 = 586.1 - 3.802 \times \text{Temperature} - 0.100 \times \text{Humidity}$	49.55
Location 3 (lat: 6.7117, long: -1.6422) 1095 Data	$CO_2 = 177.2 + 7.03 \times \text{Temperature} + 1.828 \times \text{Humidity}$	10.00

Time series plot of reported data in location 3 (lat: 6.7117, -1.6422)

5. Discussion. Carbon dioxide emissions were averagely the highest in location 3 with 508.11 ppm concentration followed by location 2 with 477.31 ppm concentration and lastly location 1 with 472.51 ppm. Location 3

Table 4.5: Summary of regression analysis of methane against temperature and humidity from the various deployed locations

Location details	Regression equation	R2 (%)
Location 1 (lat: 6.7211, long: -1.6291) 1286 Data	$CH_4 = -0.124 + 0.00833 \times \text{Temperature} + 0.00090 \times \text{Humidity}$	2.15
Location 2 (lat: 6.7113, long: -1.6306) 1246 Data	$CH_4 = -0.769 + 0.01922 \times \text{Temperature} - 0.00555 \times \text{Humidity}$	2.57
Location 3 (lat: 6.7117, long: -1.6422) 1095 Data	$CH_4 = -1.414 + 0.03560 \times \text{Temperature} - 0.00753 \times \text{Humidity}$	4.14

Table 4.6: Summary of regression analysis of temperature against humidity from the various deployed locations

Location details	Regression equation	R2 (%)
Location 1 (lat: 6.7211, long: -1.6291) 1286 Data	$\text{Temperature} = 41.0898 - 0.207153 \times \text{Humidity}$	99.26
Location 2 (lat: 6.7113, long: -1.6306) 1246 Data	$\text{Temperature} = 44.6179 - 0.254177 \times \text{Humidity}$	98.19
Location 3 (lat: 6.7117, long: -1.6422) 1095 Data	$\text{Temperature} = 44.3276 - 0.222073 \times \text{Humidity}$	98.54

also recorded the highest minimum carbon dioxide concentration (439 ppm), followed by location 2 (435.00 ppm) and the least in location 1 (421 ppm) which are all above the 2021 global carbon dioxide concentration average in the atmosphere of 414.7 ppm as observed by [23].

The average methane concentration was highest in location 1 (0.1599 ppm equivalent to 1599 ppb) followed by location 3 (0.1366 ppm equivalent to 1366 ppb) and lastly location 2 (0.1358 ppm equivalent to 1358 ppb) as shown in table 5.1. An average methane concentration recorded in all locations are slightly below the global atmospheric methane average. However, the maximum recorded methane emissions of 0.5100 ppm (5100 ppb), 0.3700 ppm (3700 ppb) and 0.4800 ppm (4800 ppb) in location 1, 2 and 3 respectively are above the 2021 global atmospheric methane average (1895.7 ppb) as observed by NOAA, (2022). A 0.08 ppm minimum methane concentration in all deployed industry locations indicates a methane background concentration of 0.08 ppm (80 ppb) within all the selected industry location and the sample site as a whole.

The reported emissions values of the MQ-135 nitrous oxide sensor were zero (0) throughout the entire deployments as shown in all the reported data as summarized also in table 4.1. This indicates that the nitrous oxide emissions are not at detectable levels to be detected by the MQ-135 nitrous oxide sensor. It is also evident according to [15]; [22]; [28] that nitrous oxide sources are mainly agriculture activity related, and was logical that the nitrous oxide emissions within all deployed industry locations within the sample site Suame Industrial Complex are zero (0).

The difference in the average temperature data reported by the DHT22 sensor and SCD-30 sensor are less than 2 ° C for location 1 and 2, and less than 2.5 ° C for location 3 as shown in table 4.2. The SCD-30 sensor reported the higher temperature values in all locations. This shows the accuracy of reported temperature data by the sensors. However, the difference in reported humidity data by DHT22 and SCD-30 sensors was less than 8 % for location 1 and 2, and approximately 10 % in location 3. The DHT22 sensor reported the much higher values of humidity in all locations. This shows the precision in the reported data by the SCD-30 and DHT22 sensors.

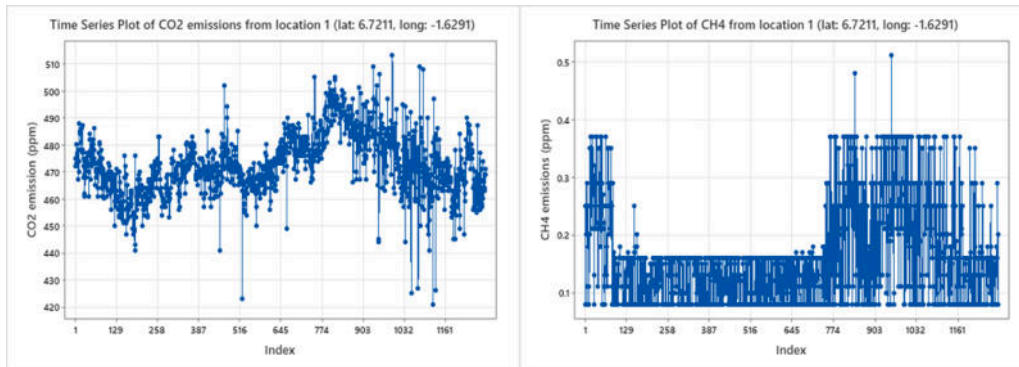


Fig. 4.1: Time series plot of reported carbon dioxide and methane emissions data from location 1 (lat: 6.7211, long: -1.6291)

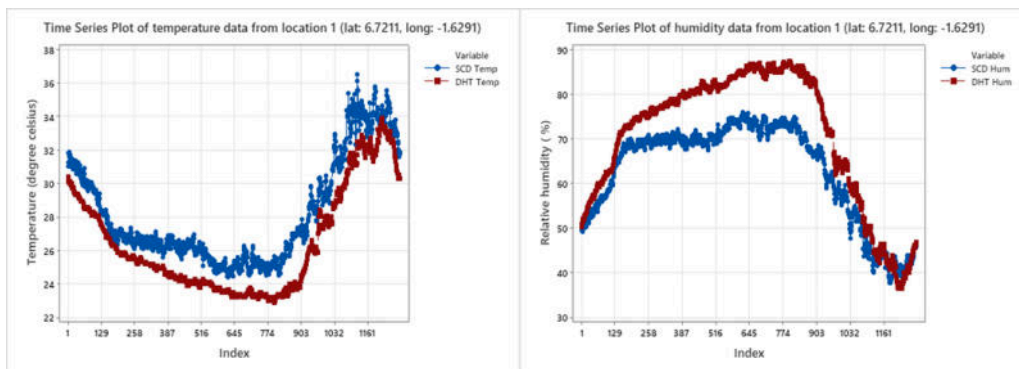


Fig. 4.2: Comparison of temperature and humidity data from location 1 (lat: 6.7211, long: -1.6291) by SCD-30 sensor and DHT22 sensor using time series plot.

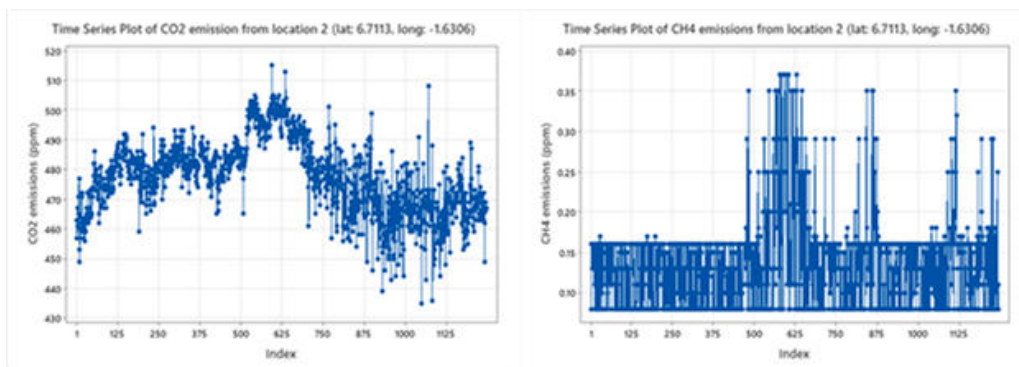


Fig. 4.3: Time series plot of reported carbon dioxide and methane emissions data from location 2 (lat: 6.7113, long: -1.6306)

As shown in table 4.3, carbon dioxide has a weaker negative correlation and weaker positive correlation with temperature and humidity respectively in location 1 and 3. However, the correlation of carbon dioxide with temperature and humidity in location 2 was moderately negative and positive of -0.704 and 0.696 respectively.

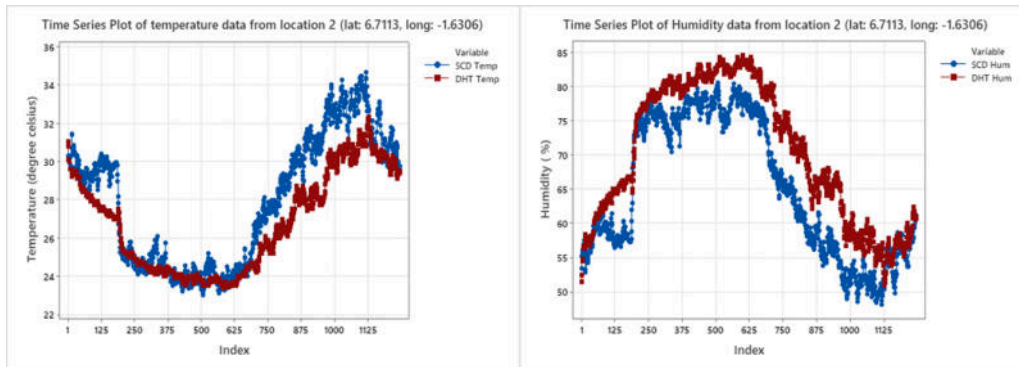


Fig. 4.4: Comparison of temperature and humidity data from location 2 (lat: 6.7113, long: -1.6306) by SCD-30 sensor and DHT22 sensor using time series plot.

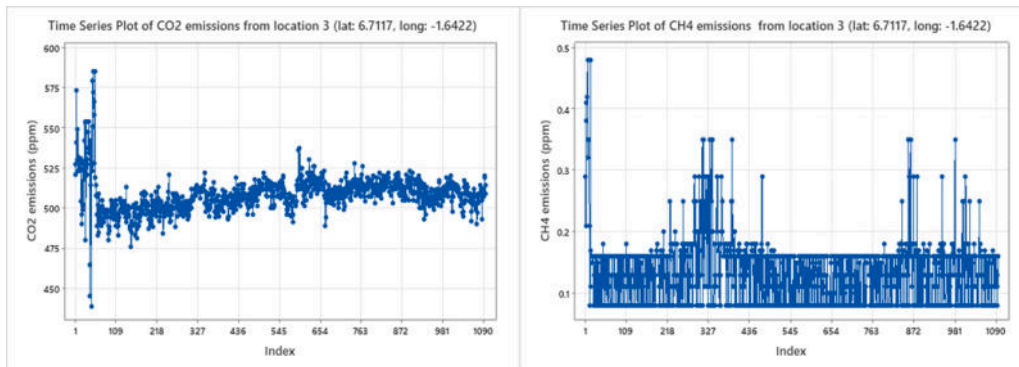


Fig. 4.5: Time series plot of reported carbon dioxide and methane emissions data from location 3 (lat: 6.7117, long: -1.6422)

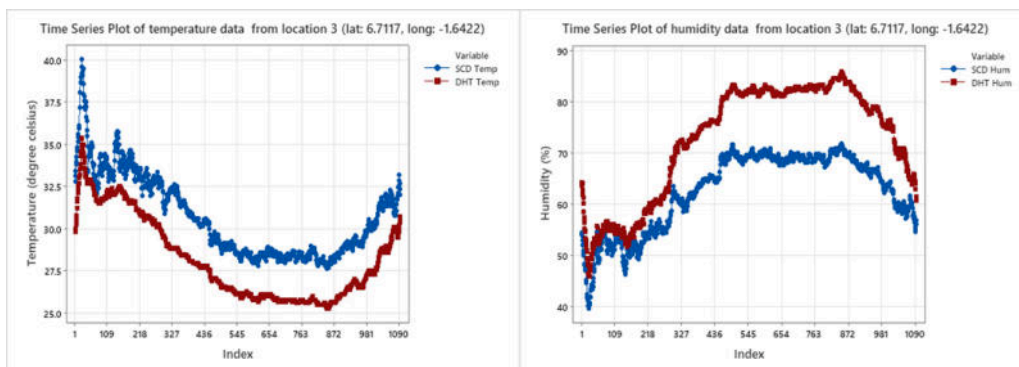


Fig. 4.6: Comparison of temperature and humidity data from location 3 (lat: 6.7117, long: -1.6422) by SCD-30 sensor and DHT22 sensor using time series plot.

This shows that either the dispersion/emissions of carbon dioxide decreases with rise in temperature and increases with increase in relative humidity. This deviate from the positive correlation of carbon dioxide and humidity as observed by [30] in their carbon dioxide emissions correlation with temperature and humidity

investigation. This also shows that the dispersion/emission of carbon dioxide is affected differently in various localities and hence much studies has to be done in various environments.

The correlation of methane with temperature and humidity was weaker (almost negligible) in all three (3) industry locations. Methane showed a negative correlation with temperature and a positive correlation with humidity in location 1 and 3. The correlation of methane in location 2 was positive with humidity and negative with temperature as also observed by [27] in their research. The variation of the correlation also suggests that, the correlation is dependent on the particular environment and much studies has to be done is GHG pollutant emissions/dispersion.

The correlation between temperature and humidity was very high in all three (3) locations with over 99 % of all the data completely correlating.

Based on the correlation analysis as shown in table 4.3 above, regression analysis was investigated with the corresponding coefficient of determination (R^2). As shown in table 4.5 above, the regression equation between methane emissions as the response variable (dependent variable) and temperature and humidity as the independent variables had the least coefficient of determination (R^2) values less than 5 % in all location. The almost negligible coefficient of determent (R^2) can be tallied with the almost negligible Pearson correlation coefficient less than 0.2 in all locations.

The coefficient of determination (R^2) of the regression equations with carbon dioxide emissions as the response variable (dependent variable), and temperature and humidity as the independent variable was less than or equal to 10 % for location 1 and 2 and approximately moderate (49.55 %) for location 2 as shown in table 4.4 above. This shows that temperature and humidity have an effect on carbon dioxide dispersion as observed in correlation research by [30, 12] in an indoor environment.

Much higher coefficient of determination (R^2) above 98 % was observed for the regression equation between temperature and humidity for all three (3) location as shown in table 4.6 as also observed by [30]. The temperature-humidity regression equation can be used in heat transfer analysis (temperature-humidity equations) as a calibration equation for temperature and humidity measurements/sensors.

The Sensiron SCD-30 carbon dioxide sensor, the DHT22 (AM2302) temperature and humidity sensor, and the MQ-4 methane sensor had a stable performance throughout its deployment. The MQ-135 nitrous oxide sensor reported zero emissions data which shows the nitrous oxide emissions are not in the detectable range of the sensor.

6. Conclusion. All the carbon dioxide emissions data collected from the various locations are above the global carbon dioxide emissions average of 414.7 ppm, hence the need for policy consideration to significantly reduce carbon dioxide emissions within the selected industrial hubs. The average methane emissions were 0.1599 ppm (1599 ppb), 0.1358 ppm (1358 ppb) and 0.1366 ppm (1366 ppb) from location 1, 2 and 3 respectively slightly below the global average of 1895.7 ppb. The maximum recorded methane emissions was 0.5100 ppm (5100 ppb), 0.3700 ppm (3700 ppb) and 0.4800 ppm (4800 ppb) which are above the global methane emissions average of 1895.7 ppb.

The use of sim800I GSM module instead of Wi-Fi provided a reliable data transmission during the deployment and solves the data transmission problem faced by the Ghana Ambient Air Quality Project (GHAir). The use of a 50 W solar panel and 19.6 Ah battery pack provided a reliable electrical power for the monitor without power blackout/outages. The selected sensors Sensiron SCD-30, MQ-4, DHT22 were able to withstand the ambient condition within the selected industry locations within Suame Industrial Complex and monitored effectively the carbon dioxide, methane, temperature and humidity.

7. Acknowledgement. The authors are thankful to KNUST Engineering Education Project (KEEPS) for providing funds for carrying out the research work.

REFERENCES

- [1] ABBAS, F. N., *Capable of Gas Sensor MQ-135 to Monitor the Air Quality with Arduino uno*, International Journal of Engineering Research and Technology, 13(10), 2020, pp.2955-2959.
- [2] ALLEN, D. T., *ScienceDirect Review Methane emissions from natural gas production and use : reconciling bottom-up and top-down measurements*, Current Opinion in chemical Engineering, 5, 2014, pp. 78-83.

- [3] AMRAGO, D., DACHNIEWSKI, M., & DANQUAH, B., *APPRENTICESHIP: TRENDS EXPERIENCES AND EXPECTATIONS OF KUMASI SUAME MAGAZINE INFORMAL INDUSTRIAL ENCLAVE IN GHANA*, History of Suame Magazine in Kumasi. Journal of Management Challenges, 1(1), 2020.
- [4] ASANTE, F. A., & AMUAKWA-MENSAH, F., *Climate Change and Variability in Ghana: Stocktaking*, Climate, 3, 2015, pp.78–99.
- [5] BENEFOH, D. T., & AMOAH, A., *Status of Monitoring Reporting Verification Scheme in Ghana (Issue November)*, 2017.
- [6] BHATTACHARJEE, D., *Design and Development of Wireless Sensor Node*, International Journal on Computer Science and Engineering, 02(07), 2010, pp.2431–2438.
- [7] BOUWMAN, A. F., HOEK, K. W. VAN DER, & OLIVIER, J. G. J., *Uncertainties in the global source distribution of nitrous oxide inventories of N₂O*, Journal of Geophysical Research, 100(D2), 1995, pp.2785–2800.
- [8] CLEMENTS, A. L., GRISWOLD, W. G., RS, A., JOHNSTON, J. E., HERTING, M. M., THORSON, J., COLLIER-OXANDALE, A., & HANNIGAN, M., *Low-Cost Air Quality Monitoring Tools: From Research to Practice (A Workshop Summary)*, Sensors, 17, 2017, pp.1–20.
- [9] DEY, T., FERREIN, A., FRAUENRATH, T., REKE, M., & SCHIFFER, S., *CO₂ Meter: A do-it-yourself carbon dioxide measuring device for the classroom* The 14th PErvasive Technologies Related to Assistive Environments Conference (PETRA), 2021, pp.1–8.
- [10] GAMELI HODOLI, C., COULON, F., & MEAD, M. I., *Applicability of factory calibrated optical particle counters for high-density air quality monitoring networks in Ghana*, Heliyon, 6(6), 2020, e04206.
- [11] GENG, Y., CHEN, W., LIU, Z., CHIU, A. S. F., HAN, W., LIU, Z., ZHONG, S., QIAN, Y., YOU, W., & CUI, X., *A bibliometric review: Energy consumption and greenhouse gas emissions in the residential sector*, Journal of Cleaner Production, 159(800), 2017, pp.301–316.
- [12] GLADYSZEWSKA-FIEDORUK, K., *Correlations of air humidity and carbon dioxide concentration in the kindergarten*, Energy & Buildings, 62, 2013, pp.45–50.
- [13] GUO, M., WANG, X., LI, J., YI, K., ZHONG, G., & TANI, H., *Assessment of Global Carbon Dioxide Concentration Using MODIS and GOSAT Data*, Sensors, 12(16368 - 16389), 2012, pp.16368–16389.
- [14] JAARMA, T., MAAT, H., RICHARDS, P., & WALS, A., *The role of materiality in apprenticeships: The case of the Suame Magazine, Kumasi, Ghana*, Journal of Vocational Education and Training, 63(3), 2011, pp.439–449.
- [15] JABLONSKA, M., & PALKOVITS, R., *Catalysis Science & Technology*, Catalysis Science and Technology, 2016, pp.1–17.
- [16] JAGATHA, J. V., KLAUSNITZER, A., CHAC, M., & LAQUAI, B., *Calibration Method for Particulate Matter Low-Cost Sensors Used in Ambient Air Quality Monitoring and Research*, Sensors, 21(3960), 2021, pp.1–27.
- [17] KARAGULIAN, F., BARBIERE, M., KOTSEV, A., SPINELLE, L., GERBOLES, M., LAGLER, F., REDON, N., CRUNAIRE, S., & BOROWIAK, A., *Review of the Performance of Low-Cost Sensors for Air Quality Monitoring*, Atmosphere, 10(506), 2019, pp.1–41.
- [18] KARAKURT, I., AYDIN, G., & AYDINER, K., *Sources and mitigation of methane emissions by sectors: A critical review*, Renewable Energy, 39(1), 2012, pp.40–48.
- [19] KEMP, A. H., & KEMP, S. A. H., *Real Time Wireless Sensor Network based Indoor Air Quality Monitoring System*, IFAC PapersOnLine, 52(24), 2019, pp.324–327.
- [20] KODOM, K., PREKO, K., & BOAMAH, D., *X-ray fluorescence (XRF) analysis of soil heavy metal pollution from an industrial area in Kumasi, Ghana.*, Soil and Sediment Contamination: An International Journal, 0383. 2012,
- [21] MANE, S. A., NADARGI, D. Y., NADARGI, J. D., ALDOSSARY, O. M., TAMBOLI, M. S., & DHULAP, V. P., *Design , Development and Validation of a Portable Gas Sensor Module: A facile Approach for Monitoring Greenhouse Gases*, Coatings, 10(1148), 2020, pp.1–11.
- [22] MOSIER, A. R., HALVORSON, A. D., & REULE, C. A., *Net Global Warming Potential and Greenhouse Gas Intensity in Irrigated Cropping Systems in Northeastern Colorado*, Journal Environmental Quality, 35, 2006, pp.1584–1598.
- [23] NOAA., *Increase in atmospheric methane set another record during 2021*, National Oceanic and Atmospheric Administration; US Department of Commerce. 2022.
- [24] ÖZDEN, Ö., DÖ, T., & KARA, S., *Assessment of ambient air quality in Eski şehir , Turkey*, Environment International, 34, 2008, pp.678–687.
- [25] SEWOR, C., A. OBENG, A., & AMEGAH, K., *Commentary: The Ghana Urban Air Quality Project (GHAir): Bridging air pollution data gaps in Ghana*, Clean Air Journal, 31(1), 2021, pp.1–2.
- [26] SHI, R., & CONRAD, S. A., *Correlation and regression analysis*, Annals of Allergy, Asthma and Immunology, 103(4), 2009, pp.S35–S41.
- [27] SRIVASTAVA, R. K., SARKAR, S., & BEIG, G., *Correlation of Various Gaseous Pollutants with Meteorological Parameter (Temperature, Relative Humidity and Rainfall)*, GLOBAL JOURNAL OF SCIENCE FRONTIER RESEARCH: H ENVIRONMENT & EARTH SCIENCE, 14(6), 2014, pp.57–65.
- [28] WUEBBLES, D. J., *Nitrous Oxide: No Laughing Matter*, Science, 56(2009), 2014, pp.56–57. <https://doi.org/10.1126/science.1179571>
- [29] YEEBO, Y., *Suame Magazine Photo Essay: Suame Magazine*, Humanity: An International Journal of Human Rights, Humanitarianism, and Development, 7(1), 2016, pp.111–121.
- [30] YULIANG, L., XIANG, N., YUANXI, W., & WEI, Z., *Study on effect of temperature and humidity on the CO₂ concentration measurement Study on effect of temperature and humidity on the CO₂ concentration measurement*, IOP Conference Series: Earth and Environmental Science PAPER, 81, 2017, pp.1–6.
- [31] ZHANG, H., ZHANG, J., WANG, R., HUANG, Y., ZHANG, M., SHANG, X., & GAO, C., *Smart carbon monitoring platform under IoT-Cloud architecture for small cities in B5G*, Wireless Networks, 2, 2021, pp.1–17.
- [32] JEFFRY, L., YIN, M., NOMANBHAY, S., MOFIJUR, M., MUBASHIR, M., & LOKE, P., *Greenhouse gases utilization: A review*,

- Fuel, 301, 2021.
- [33] HERZOG, T., *World Greenhouse Gas Emissions*, 2009.
- [34] KUMAR, A., SINGH, P., RAIZADA, P., & MUSTANSAR, C., *Science of the Total Environment Impact of COVID-19 on greenhouse gases emissions: A critical review*, Science of the Total Environment, 806, 2022.
- [35] BOESCH, H., LIU, Y., TAMMINEN, J., YANG, D., PALMER, P. I., LINDQVIST, H., CAI, Z., CHE, K., NOIA, A. DI, FENG, L., HAKKARAINEN, J., IALONGO, I., KALAITZI, N., KARPPINEN, T., KIVI, R., KIVIMÄKI, E., PARKER, R. J., PREVAL, S., WANG, J., ... CHEN, H., *Monitoring Greenhouse Gases from Space*, Sensors, 13, 2021.
- [36] LAMB, W. F., WIEDMANN, T., TUBIELLO, F. N., SALVATORE, M., LAMB, W. F., WIEDMANN, T., PONGRATZ, J., ANDREW, R., CRIPPA, M., OLIVIER, J. G. J., WIEDENHOFER, D., MATTIOLI, G., KHOURDAJIE, A. AL, & HOUSE, J., *A review of trends and drivers of greenhouse gas emissions by sector from 1990 to 2018*, Environmental Research Letters, 16, 2018.
- [37] AHMAD, M., BEDDU, S., BINTI ITAM, Z., & ALANIMI, F. B. I. , *State of the art compendium of macro and micro energies*, Advances in Science and Technology Research Journal, 13, 2019.
- [38] FLERLAGE, H., VELDERS, G. J. M., & BOER, J. DE., *Chemosphere A review of bottom-up and top-down emission estimates of hydrofluorocarbons (HFCs) in different parts of the world*, Chemosphere, 283, 2021.
- [39] CREUTZIG, F., POPP, A., PLEVIN, R., LUDERER, G., MINX, J., & EDENHOFER, O., *Reconciling top-down and bottom-up modelling on future bioenergy deployment*, Nature Climate Change, 2(5), 2021, pp. 320-327.
- [40] FRIEDRICH, E., & TROIS, C., *Quantification of greenhouse gas emissions from waste management processes for municipalities – A comparative review focusing on Africa*, Waste Management, 31(7), 2011, pp. 1585–1596.
- [41] YODI, I. W. K. S., & AFIFAH, A. S., *Estimation of Green House Gas (GHG) emission at Telaga Punggur landfill using triangular, LandGEM, and IPCC methods*, Journal of Physics, 1452, 2020, pp. 1-8.
- [42] MORRISON, S. R. , *Selectivity in semiconductor gas sensors*, Sensors and Actuators, 12, 1987, pp. 425-440.
- [43] SBERVEGLIERI, G. , *Recent developments in semiconducting thin-film gas sensors*, Sensors and Actuators, 23, 1995, pp. 103-109.
- [44] SAKAKURA, T., CHOI, J., & YASUDA, H., *Transformation of Carbon Dioxide*, Chemical Reviews, 107(6), 2007, pp. 2365–2387.
- [45] CRABTREE, R. H., *Aspects of Methane Chemistry*, Chemical Reviews, 1994, pp. 987-1007.
- [46] KOESTOER, R. A., PANCASAPUTRA, N., & ROIHAN, I., *A sirelativemple calibration methods of humidity sensor DHT22 for tropical climates based on Arduino data acquisition system*, AIP Conference Proceedings, 2019, pp. 1-8.
- [47] MIHAI, B. , *How to use the DHT22 sensor for measuring temperature and humidity with the Arduino Board*, DE GRUYTER OPEN, 2016, pp. 22-25.
- [48] ADHIWIBOWO, W., DARU, A. F., & HIRZAN, A. M., *Temperature and Humidity Monitoring Using DHT22 Sensor and Cayenne API*, TRANSFORMTIKA, 17(2), 2020, pp. 209-214.

Edited by: Vinoth Kumar

Received: Aug 16, 2022

Accepted: Nov 29, 2022